


## ORIGINAL ARTICLE

# Interferon-expressing oncolytic adenovirus + chemoradiation inhibited pancreatic cancer growth in a hamster model

Shuhei Shinoda<sup>1,2</sup>  | Nikita S. Sharma<sup>1</sup> | Naohiko Nakamura<sup>1</sup> | Kazuho Inoko<sup>1</sup> | Mizuho Sato-Dahlman<sup>1,3</sup> | Paari Murugan<sup>4</sup> | Julia Davydova<sup>1,3</sup> | Masato Yamamoto<sup>1,3,5</sup>

<sup>1</sup>Department of Surgery, University of Minnesota, Minneapolis, MN, USA

<sup>2</sup>Department of Gastroenterology and Hepatology, Yamaguchi University Graduate school of Medicine, Yamaguchi, Japan

<sup>3</sup>Masonic Cancer Center, University of Minnesota, Minneapolis, MN, USA

<sup>4</sup>Department of Laboratory Medicine and Pathology, University of Minnesota, Minneapolis, MN, USA

<sup>5</sup>Institute of Molecular Virology, University of Minnesota, Minneapolis, MN, USA

## Correspondence

Masato Yamamoto, Department of Surgery, University of Minnesota, Moost 11-216, 515 Delaware St SE, Minneapolis, MN 55455, USA.

Email: [yamam016@umn.edu](mailto:yamam016@umn.edu)

## Funding information

National Cancer Institute, Grant/Award Number: P30CA077598-22S3, R01CA196215, R01CA228760 and R01CA276480

## Abstract

Past clinical trials of adjuvant therapy combined with interferon (IFN) alpha, fluorouracil, cisplatin, and radiation improved the 5-year survival rate of pancreatic ductal adenocarcinoma (PDAC). However, these trials also revealed the disadvantages of the systemic toxicity of IFN and insufficient delivery of IFN. To improve efficacy and tolerability, we have developed an oncolytic adenovirus-expressing IFN (IFN-OAd). Here, we evaluated IFN-OAd in combination with chemotherapy (gemcitabine + nab-paclitaxel) + radiation. Combination index (CI) analysis showed that IFN-OAd + chemotherapy + radiation was synergistic (CI < 1). Notably, IFN-OAd + chemotherapy + radiation remarkably suppressed tumor growth and induced a higher number of tumor-infiltrating lymphocytes without severe side toxic effects in an immunocompetent and adenovirus replication-permissive hamster PDAC model. This is the first study to report that gemcitabine + nab-paclitaxel, the current first-line chemotherapy for PDAC, did not hamper virus replication in a replication-permissive immunocompetent model. IFN-OAd has the potential to overcome the barriers to clinical application of IFN-based therapy through its tumor-specific expression of IFN, induction of antitumor immunity, and sensitization with chemoradiation. Combining IFN-OAd with gemcitabine + nab-paclitaxel + radiation might be an effective and clinically beneficial treatment for PDAC patients.

## KEYWORDS

interferon alpha, nab-PTX, oncolytic adenovirus, oncolytic virus, pancreatic cancer

**Abbreviations:** 5-FU, fluorouracil; ADP, adenoviral death protein; BED, biologically effective dose; BRPC, borderline resectable pancreatic cancer; CI, combination index; CR, chemotherapy + radiation; CRV, chemotherapy + radiation + IFN-OAd; CV, chemotherapy + IFN-OAd; FOLFIRINOX, combination of 5-FU, oxaliplatin, and irinotecan; GEM, gemcitabine; HE, hematoxylin and eosin; IFN, interferon alpha; IFN-OAd, IFN expressing oncolytic adenovirus; LAPC, locally advanced and unresectable pancreatic cancer; MTS, 3-(4,5-dimethylthiazol-2-yl)-5-(3-carboxymethoxyphenyl)-2-(4-sulfophenyl)-2H-tetrazolium, inner salt; nab-PTX, nab-paclitaxel; OAd, oncolytic adenovirus; PDAC, pancreatic ductal adenocarcinoma; PFU, plaque forming unit; PTX, paclitaxel; RGD-4C, Arginine-Glycine-Aspartic; RV, radiation + IFN-OAd; TIL, tumor-infiltrating lymphocyte; VP, viral particle.

This is an open access article under the terms of the [Creative Commons Attribution-NonCommercial](https://creativecommons.org/licenses/by-nc/4.0/) License, which permits use, distribution and reproduction in any medium, provided the original work is properly cited and is not used for commercial purposes.

© 2023 The Authors. *Cancer Science* published by John Wiley & Sons Australia, Ltd on behalf of Japanese Cancer Association.

## 1 | INTRODUCTION

Pancreatic ductal adenocarcinoma (PDAC) is one of the most devastating cancers.<sup>1,2</sup> Despite recent advances in cancer diagnostics, effective screening is not available for PDAC, and most patients already have locally advanced (30%–35%) or metastatic (50%–55%) disease at diagnosis.<sup>2</sup> In the United States, Siegel et al. estimated the 5-year survival rate of PDAC to be 9%.<sup>3</sup> PDAC is expected to become the second leading cause of cancer-related mortality by 2030.<sup>2</sup> Neoadjuvant chemotherapy with or without radiation with subsequent surgery is a standard treatment for locally advanced and unresectable pancreatic cancer (LAPC), including borderline resectable pancreatic cancer (BRPC).<sup>2</sup> In these groups of patients, neoadjuvant treatment of local disease will benefit both resectability and prognosis, but the consistently poor prognosis of those even with neoadjuvant chemotherapy indicates that novel therapeutics for surgery are desperately needed.

Type I interferon (IFN) is a cytokine with multiple functions, including antitumor activity, immunomodulation, and direct induction of apoptosis.<sup>4,5</sup> It is a particularly attractive agent for combination therapy because it sensitizes many cancers to a variety of chemotherapy and radiation regimens.<sup>4–7</sup> Picozzi et al.<sup>8</sup> reported that clinical trials of adjuvant therapy combined with IFN, fluorouracil (5-FU), cisplatin, and radiation improved the 5-year survival rate of patients with PDAC by 35%. At the same time, trials of IFN alpha-based chemoradiation revealed problems impairing its broad clinical implementation for PDAC patients, including systemic toxicity that resulted in a high dropout rate and insufficient delivery of IFN to the tumor.<sup>8–11</sup>

In various cancers, including PDAC, oncolytic adenovirus (OAd) has shown strong oncolytic effects.<sup>12,13</sup> It selectively replicates and spreads in the tumor to induce immunogenic cell death, which evokes a strong antitumor immune response. Furthermore, a transgene placed in a specific location of OAd induces massive and selective expression in the target cancer cells.<sup>13</sup> IFN expression from OAd enables both tumor suppression and massive local IFN expression in the tumor. In addition, OAd blocks the IFN response by inhibiting cytoplasmic signaling pathways and the activation of IFN-stimulated genes.<sup>14,15</sup> This means that IFN expression does not hamper adenovirus replication, and OAd is a suitable vector for the expression of IFN.

We have reported that the IFN-expressing OAd (IFN-OAd) improved the oncolytic effect against PDAC cells mediated by IFN overexpression in both a human pancreatic cancer xenograft model in mice<sup>16</sup> and a hamster syngeneic tumor model.<sup>17</sup> We also clarified that IFN-OAd potentiated the cytotoxicity/antitumor effect of radiation *in vitro* and *in vivo*.<sup>18</sup> A recent case-control matched analysis of LAPC reported that neoadjuvant chemoradiation therapy is associated with and disease-free survival compared with neoadjuvant chemotherapy alone.<sup>19</sup> We improved pathologic surrogates hypothesize that combining IFN-OAd with chemoradiation will be an effective and clinically beneficial treatment for LAPC and BRPC patients. To achieve good clinical translatability,

we believe it is important to choose the current first-line chemotherapy option for PDAC. In the clinical setting, gemcitabine (GEM)+nab-paclitaxel (nab-PTX) has good survival benefits compared with a single-agent GEM for patients with advanced PDAC.<sup>20</sup> As of 2022, GEM+nab-PTX and the combination of 5-FU, oxaliplatin, and irinotecan (FOLFIRINOX) are valid first-line options for PDAC.<sup>2</sup> Based on this background, in this study, we evaluated the antitumor potential of IFN-OAd in combination with GEM+nab-PTX+radiation using an immunocompetent and replication permissive hamster PDAC model.

## 2 | MATERIALS AND METHODS

### 2.1 | Cell lines

The Syrian hamster pancreatic cancer cell line HP-1 was provided by Dr. M. A. Hollingsworth (University of Nebraska, Omaha, NE). HP-1 cells were cultured in DMEM (Mediatech). Cells were supplemented with FBS (10% for cell line wake-up, 5% for culture maintenance) and a 1% penicillin–streptomycin mixture (100 IU/mL and 100 µg/mL, respectively) and were maintained as adherent monolayers at 37°C in a humidified incubator with 5% CO<sub>2</sub>.

### 2.2 | Adenoviral vectors

The IFN-OAd was based on adenovirus type 5 and overexpresses adenoviral death protein (ADP), as we have previously described.<sup>17,18</sup> Hamster IFN alpha gene (kindly provided by Dr. Aoki,<sup>21</sup> National Cancer Research Institute, Tokyo, Japan) was placed in the adenovirus E3 region.<sup>22</sup> To increase the infectivity of the virus in hamster pancreatic cancer cells, an arginine-glycine-aspartic motif (RGD-4C) was incorporated in the HI-loop of IFN-OAd.<sup>23</sup> Virus purification, titration, and structure confirmation were performed as described previously.<sup>16,24</sup> All viruses were propagated in the 911 cell line, purified by double cesium chloride density gradient ultracentrifugation, and dialyzed against PBS with 10% glycerol. The vectors were titrated by plaque forming unit (PFU) assay, and the viral particle (VP) number was measured spectrophotometrically.

### 2.3 | Reagents

Gemcitabine (GEM) and paclitaxel (PTX) were purchased from Athenex, while Abraxane (nab-PTX) was purchased from Celgene. Drugs were diluted according to the manufacturers' protocols.

### 2.4 | Analysis of viral replication

HP-1 cells in six-well plates ( $1 \times 10^6$  cells per well) were infected with viruses (0.25, 2.5, 25 VP/cell). Twenty-four hours after infection,

GEM (0, 2.5, and 10 nM) and/or PTX (0, 2.5, and 10 nM) were added to each well. Then, the growth medium was harvested at 7 days after infection to assess progeny production. The total viral copy number was analyzed with the E4 primers by SYBRGreen quantitative PCR (qPCR) as described previously.<sup>25</sup>

## 2.5 | Cell viability assay

For quantitative analyses, 5000 cells/well were plated in 96-well plates and infected with IFN-OAd (0, 0.25, 2.5, and 25 VP/cell) (Day 0). Twenty-four hours after infection, GEM (0, 2.5, and 10 nM) and PTX (0, 2.5, and 10 nM) were subsequently added to each well. A viability assay was performed on Days 4 and 7 with CellTiter-96 Aqueous One-Solution Cell Proliferation Assay MTS reagent (Promega) according to the manufacturer's instructions as described previously.<sup>18</sup>

## 2.6 | Radiation

Radiation in vitro and in vivo was performed using the X-RAD 320 X-ray system (Precision Xray). The X-ray radiation platform was positioned 50 cm from the bottom of the machine, and Filter 1 (2.0 mm Aluminum/Half Value Layer 1.0 mm Cu) was used. To determine the dose for radiotherapy in the experiment, the biologically effective dose (BED) based on the "linear quadratic model" has been used.<sup>26</sup> As described in a previous paper,<sup>18</sup> we set the radiation dosage as an 8 Gy single fraction for in vivo experiments. The BED of the 8 Gy single fraction is 14.4.

## 2.7 | Colony formation assay

Next,  $1.0 \times 10^6$  cells were seeded in 75-cm<sup>2</sup> flasks and incubated at 37°C in a humidified 5% CO<sub>2</sub> incubator.

After 24 h incubation, cells were infected with IFN-OAd (0.0625, 0.3, and 0.625 VP/cell) (Day 0). On the following day, cells were irradiated (0.625, 1.25, and 2.5 Gy), trypsinized with 0.25% Trypsin-EDTA, counted, serially diluted, and plated in 10-cm culture dishes with standard media (DMEM with 10% FBS, 1% penicillin/streptomycin). Plates receiving chemotherapy as part of the treatment had 2.5 nM GEM plus 2.5 nM PTX added to the media at the time of plating. Media was replaced in all plates every 3 days. On Day 14, the plates were fixed with 4% formalin for 1 hour, stained with 1% methylene blue overnight, washed with PBS three times, and allowed to air dry. Colonies were counted, and the following formula was used to estimate the assay results:

Cell survival fraction = Number of colonies / (Number of plated cells × Plating efficiency)

Plating efficiency = Number of colonies in untreated control / Number of plated cells in untreated control.

## 2.8 | Combination index analysis

Calculation of the combination index (CI) to determine synergism (CI < 1), antagonism (CI > 1), or additive effect (CI = 1) between virus, chemotherapy, and radiation was performed using Compusyn software.<sup>27</sup> The quantification of the cytotoxicity of combination treatments was determined by CFA, and the killing effect was entered as the combo therapies in Compusyn. The final report with CI was generated using a nonconstant ratio between therapies.

## 2.9 | In vivo analysis in a Syrian hamster model

All procedures were carried out according to protocols approved by the Institutional Animal Care and Use Committee (IACUC) of the University of Minnesota. Male and female Syrian golden hamsters (*Mesocricetus auratus*, HsdHan: AURA; 6–7 weeks of age) were obtained from Harlan Sprague Dawley. Before the procedures, the animals were anesthetized with isoflurane. Hamster pancreatic cancer cells (HP-1,  $2 \times 10^6$  cells in 100 μl of PBS) were subcutaneously inoculated into the flank of each animal. The tumor diameter was measured twice per week with calipers. The tumor volume was calculated using the following formula: estimated tumor volume = (shortest diameter<sup>2</sup> × longest diameter) / 2. When the average estimated tumor volume reached 200 mm<sup>3</sup>, the hamsters were divided into four groups: Control ( $n=4$ ), CR ( $n=10$ ), V ( $n=6$ ), and CRV ( $n=5$ ) groups. A single dose ( $2.5 \times 10^9$  PFU/tumor) of virus or vehicle alone (PBS) was injected into the tumors on Day 0. Radiation (8 Gy single fraction) was performed on Day 3. Intraperitoneal injections of 20 mg/kg GEM plus 2 mg/kg nab-PTX were given on Days 3, 6, 10, 13, 17, and 20. At the end of the experiments, the hamsters were killed in accordance with the guidelines of the IACUC of the University of Minnesota. Blood samples were collected simultaneously during tumor removal. Serum biochemistries were analyzed by IDEXX BioAnalytics. The tumors were excised and processed for HE staining to assess the TIL. We asked a board-certified anatomic pathologist to assess the TIL on HE sections based on the International Immuno-Oncology Biomarker Working Group guidelines for TIL assessment in invasive breast carcinoma.<sup>28,29</sup> Briefly, after choosing the random three areas from both the intratumoral and marginal areas, we scored the average TIL. TIL was reported as a percentage. Necrotic areas were excluded.

In a separate experiment under the same conditions, the hamsters were killed on Day 7. The DNA was purified from whole frozen tumors using a DNeasy Blood and Tissue Kit (Qiagen), and the adenoviral DNA copy number of the E4 region was quantified by qPCR starting from 100 ng DNA.

The expression of adenoviral hexon protein in the tumor on Day 7 was analyzed by immunostaining as described previously.<sup>30</sup> Briefly, the slices fixed by 10% formaldehyde were stained with anti-hexon goat polyclonal antibody, FITC conjugated (dilution 1:10, AB1056F, Sigma-Aldrich). To assess the general condition and fibrosis of tumors, we also performed HE and Masson's trichrome staining, showing a similar region of interest. All slides were scanned using a Leica DM5500 B microscope (Leica Microsystems).

## 2.10 | Statistical methods

Statistical significance was determined using Student's *t* test. JMP 9 statistical software (SAS Institute) was employed in the analysis. Results are expressed as mean  $\pm$  standard deviation, and differences with  $p < 0.05$  were considered statistically significant.

## 3 | RESULTS

### 3.1 | Replication of IFN-OAd with gemcitabine and/or paclitaxel

We assessed how GEM and paclitaxel (PTX) affect the replication of IFN-OAd (Figure 1A) in HP-1 cells, one of the hamster pancreatic cancer cell lines. IFN-OAd was based on adenovirus type 5 and overexpresses ADP as we have previously described.<sup>17,18</sup> Hamster IFN alpha gene was placed in the adenovirus E3 region.<sup>22</sup> To increase the infectivity of the virus in hamster pancreatic cancer cells, the RGD-4C motif was incorporated in the HI-loop of IFN-OAd.<sup>23</sup> HP-1 cells were infected with viruses (0.25, 2.5, and 25 VP/cell). PBS (Without chemo), GEM (GEM only: 2.5 or 10 nM GEM), PTX (PTX only: 2.5 nM or 10 nM PTX), and GEM+PTX (2.5 nM GEM+2.5 nM PTX or 10 nM GEM+10 nM PTX) were subsequently added 24 h after infection. Seven days after infection, the PTX only group had a significantly higher ( $\geq 1.2$  times) VP number compared to the without chemo group (Figure 1B–E). Furthermore, the GEM+PTX group had a significantly higher VP number compared to the GEM only group. These data indicated that PTX enhanced the replication of IFN-OAd.

### 3.2 | In vitro cell viability analysis

To quantitatively analyze the cytotoxicity of chemotherapeutics when combined with IFN-OAd, the cell viability of HP-1 cells treated with IFN-OAd and chemo (GEM+PTX) was assessed using the MTS assay (Figure 2A,B). Twenty-four hours after infection, chemo drugs were added to each well. On Days 4 and 7, we assessed the cell viability by 3-(4,5-dimethylthiazol-2-yl)-5-(3-carboxymethoxyphenyl)-2-(4-sulfophenyl)-2H-tetrazolium, inner salt (MTS) assay. IFN-OAd with chemo suppressed the HP-1 cell proliferation in a dose-dependent manner.

### 3.3 | IFN-OAd potentiated the inhibition of colony formation by chemotherapy and radiation

The colony formation assay was employed to assess the radiosensitivity of cancer cells. To characterize the interaction among the chemo, radiation, and IFN-OAd, we performed a synergy analysis using the colony formation assay (Figure 2C–E) as described previously.<sup>18</sup> Briefly, cells were infected with IFN-OAd (0.0625, 0.300 and 0.625 VP/cell). Twenty-four hours after infection, cells were irradiated (0.625 Gy) and received chemotherapy (2.5 nM). After 14 days, colonies were counted. Calculation of the CI to determine synergism ( $CI < 1$ ), antagonism ( $CI > 1$ ), or additive effect ( $CI = 1$ ) among virus, chemotherapy, and radiation was performed using Compusyn software.<sup>27</sup> The triple-therapy regimen (chemotherapy+ radiation+ IFN-OAd: CRV) showed remarkable inhibition of colony formation regardless of the VP number of IFN-OAd. The CI analysis showed that CRV was synergistic ( $CI < 1$ ) (Table 1). Of note, CRV was significantly more effective than chemotherapy+ radiation (CR), chemotherapy+ IFN-OAd (CV), and radiation+ IFN-OAd (RV) in the colony formation assay.

### 3.4 | Chemotherapy + radiation + IFN-OAd suppressed tumor growth in a hamster syngeneic subcutaneous tumor model without serious side effects

Tumor growth inhibition of the combined treatment of CRV against HP-1 cells was assessed in the hamster syngeneic subcutaneous tumor model. HP1 cells were injected subcutaneously into the backs of the Syrian hamsters. When the tumor volume reached 200 mm<sup>3</sup>, we performed intratumoral viral injection (IFN-OAd:  $2.5 \times 10^9$  plaque forming unit [PFU]). Three days after virus injection, a clinically feasible fraction of 8 Gy was given. We also intraperitoneally injected GEM (20 mg/kg)+ nab-PTX (2 mg/kg) twice weekly. The hamsters were killed at the end of this experiment (Figure 3A). CR, IFN-OAd only (V), and CRV did not show any serious side effects, such as weight loss (Figure 3B) or altered serum biochemistries (total protein, albumin, total bilirubin, AST, ALT, BUN, and creatinine; Table 2). The average tumor volumes on Day 21 of the control, CR, V, and CRV were  $2027 \pm 1296$ ,  $908 \pm 849$ ,  $767 \pm 593$ , and  $202 \pm 161$  mm<sup>3</sup>,<sup>3</sup> respectively (Figure 3C–H). It is noteworthy that CRV significantly suppressed tumor growth without serious side toxicity compared to CR.

### 3.5 | Chemotherapy + radiation + IFN-OAd induced higher number of tumor-infiltrating lymphocytes

Hamster syngeneic subcutaneous tumor (HP-1 cells) were excised and processed on Day 21 to assess the tumor-infiltrating lymphocyte (TIL). Antibodies for hamster cells were limited, and we asked

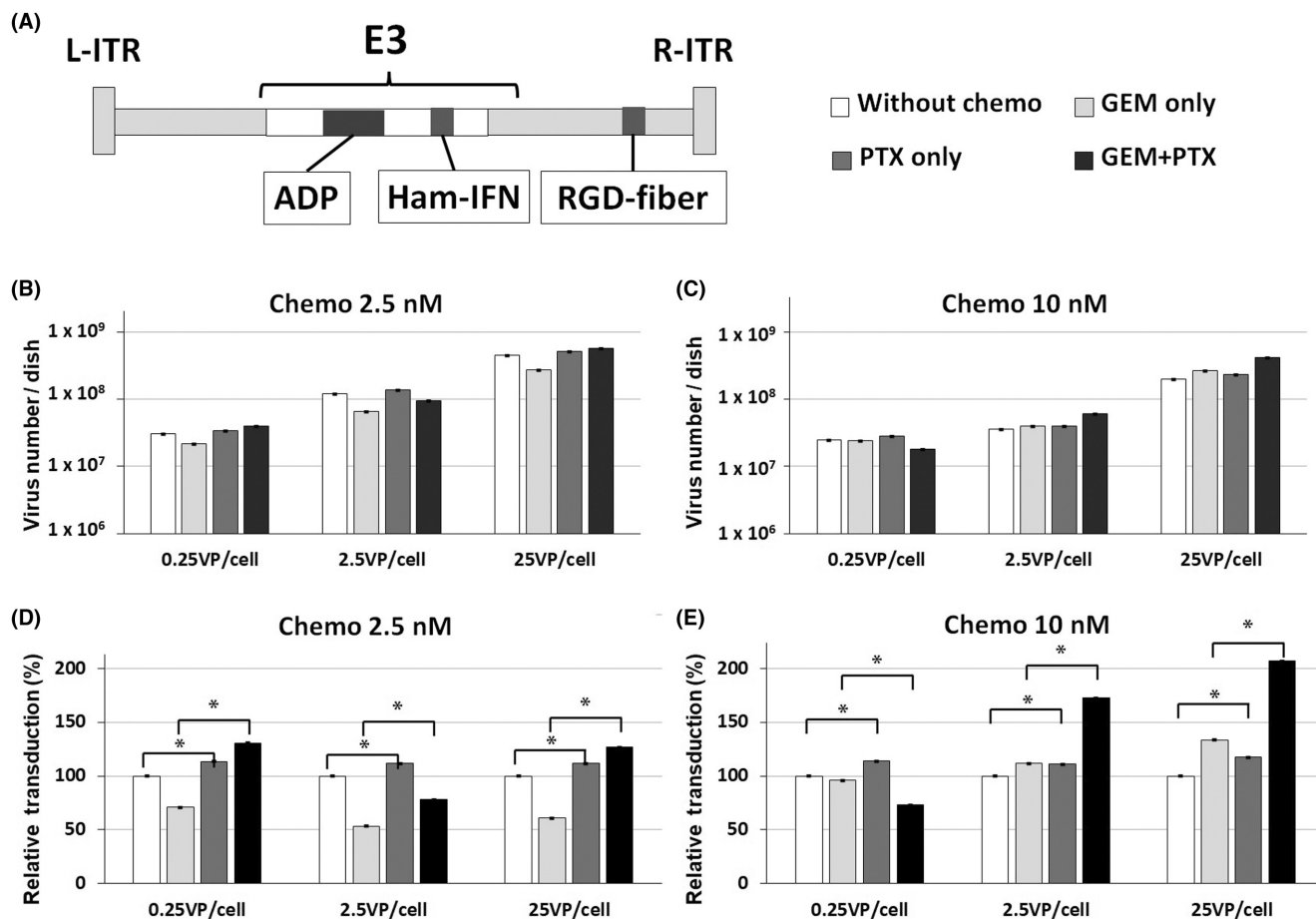


**FIGURE 1** Viral replication of the interferon (IFN)-expressing oncolytic adenovirus (IFN-OAd) combined with chemotherapy. (A) Structure of the IFN alpha-expressing oncolytic adenovirus (IFN-OAd). IFN-OAd is a wild-type replication oncolytic adenovirus expressing the hamster IFN alpha gene from the adenoviral E3 region. (B–E) Viral replication of IFN-OAd with gemcitabine (GEM) and paclitaxel (PTX) in vitro. HP-1 cells were infected with IFN-OAd. Twenty-four hours after infection, PBS (Without chemo), GEM (GEM only: 2.5 or 10 nM GEM), PTX (PTX only: 2.5 nM or 10 nM PTX), and GEM+PTX (2.5 nM GEM+2.5 nM PTX or 10 nM GEM+10 nM PTX) were added to each well. The viral copy number was measured by quantitative PCR (qPCR) on Day 7. The results are shown as E4 copy number per dish and ratio compared to without chemo ( $n=3$ ). Data are presented as mean  $\pm$  standard deviation ( $n=3$ ,  $*p<0.05$ ). ADP, adenoviral death protein; Ham-IFN, hamster interferon alpha; L-ITR, left inverted terminal repeat; RGD, RGD-4C (arginine-glycine-aspartic) motif; R-ITR, right inverted terminal repeat.

the pathologist to assess the TIL in both the intratumoral and the marginal area on hematoxylin and eosin (HE) sections based on the standardized methodology (Figure 4A,B).<sup>28,29</sup> CRV significantly increased the score of TIL in both of the intratumoral and the marginal area compared to CR.

### 3.6 | Chemotherapy + radiation did not hamper virus replication in vivo

To investigate the spread and the replication of the virus, we performed a separate experiment in hamster syngeneic subcutaneous tumors with the same setup, and the tumor samples on Day 7 were assessed for viral structural protein (hexon) staining (Figure 5A) and viral copy number (Figure 5B). The staining of hexon in the tumor specimens on Day 7 after virus injection showed widespread

distribution in the tumors treated with V. CRV showed broad necrotic area and stronger fibrosis due to the treatment effect on HE and Masson's trichrome stained slides. Hexon expression of CRV was mainly located in the area residual tumor cells exist, not in the necrotic area. Furthermore, CRV showed noninferiority in terms of the virus copy number in tumors compared to V. These data indicated that CRV suppressed tumor growth without hampering the IFN-OAd replication in hamster syngeneic subcutaneous tumors.

## 4 | DISCUSSION

In this study, we focused on the antitumor potential of IFN-OAd in combination with GEM+nab-PTX+radiation. As we previously reported, IFN-OAd monotherapy has already shown cytotoxicity for HP1 cells in a dose-dependent manner,<sup>17,18</sup> and IFN-OAd potentiated

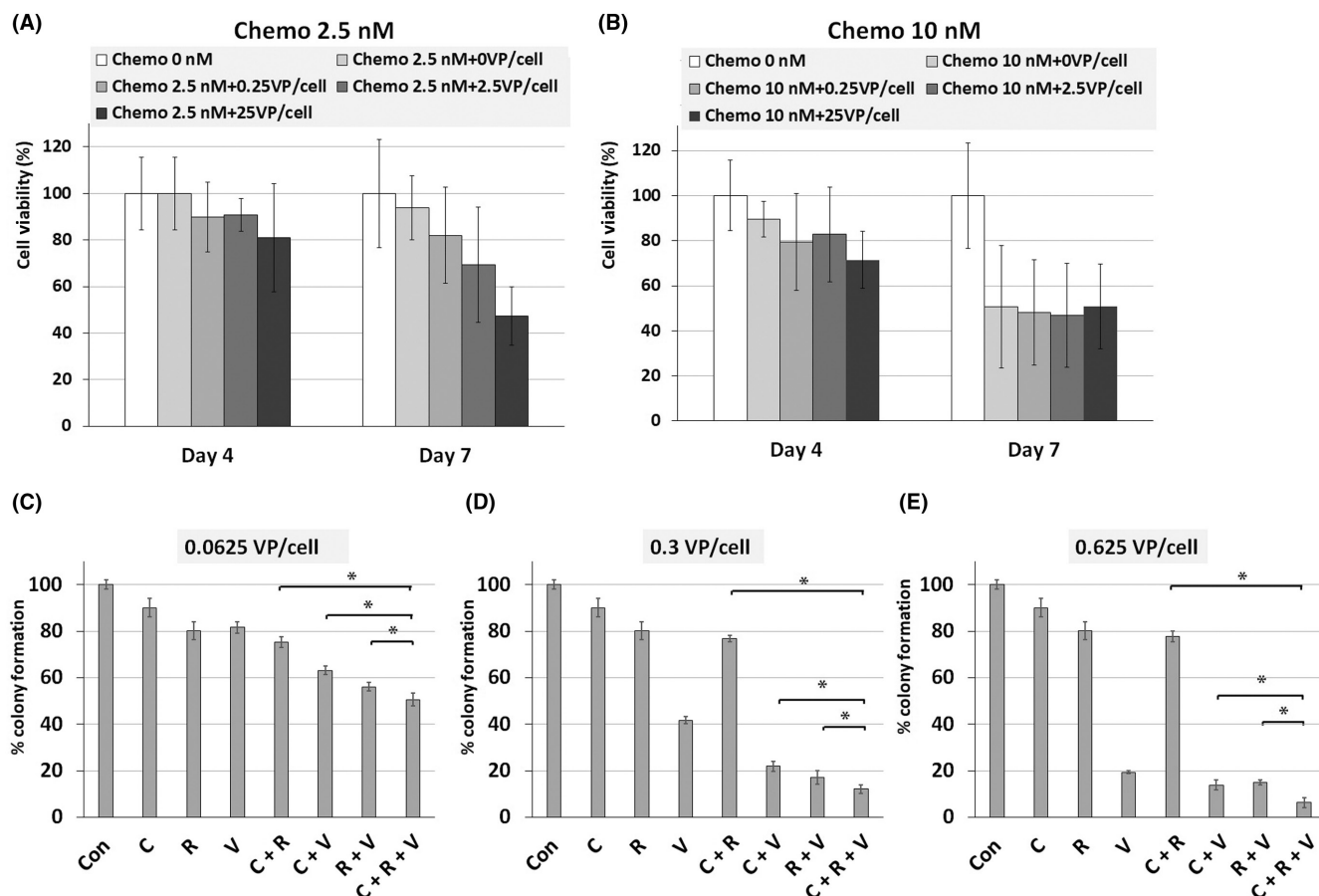


**FIGURE 2** Cell viability assay and colony formation assay of interferon (IFN)-expressing oncolytic adenovirus (IFN-OAd) combination with chemotherapy and radiation therapy. (A, B) Cell viability assay of IFN-OAd with chemotherapy. HP-1 cells were infected with IFN-OAd (Day 0). Twenty-four hours after infection, gemcitabine (GEM) and paclitaxel (PTX) were added. On Days 4 and 7, cell viability was assessed ( $n=3$ ). (C-E) Colony formation assay of IFN-OAd combination with GEM+PTX and radiation therapy. HP-1 cells were infected with IFN-OAd (Day 0), and on the following day, cells were irradiated and plated. GEM+PTX was also added. On Day 14, colonies were counted. Data are presented as mean  $\pm$  standard deviation ( $n=3$ ,  $*p<0.05$ ). C, chemotherapy; Con, control; R, radiation therapy; V, IFN-OAd.

the cytotoxicity of radiation in vitro and in vivo experiments.<sup>18</sup> Other groups also reported the good combined effect of OAd and radiation in several cancers.<sup>31,32</sup> In contrast, how each chemotherapy drug affects the OAd replication has not been elucidated well. In fact, GEM, a nucleoside analog, has a high possibility of inhibiting viral replication because gemcitabine prevents DNA chain elongation.<sup>33</sup> In contrast, several publications reported the enhancement of the efficacy of gemcitabine with adenovirus-based vectors for treating PDAC in in vivo experiments.<sup>34,35</sup> We reported that GEM monotherapy showed antitumor effects for hamster pancreatic cancer cell lines in a dose-dependent manner, and IFN-OAd accentuated the cytotoxic effect of GEM.<sup>18</sup> The inhibition of OAd replication by GEM may depend on the experimental design, including the cell line, exposure time, VP numbers, and GEM concentration. nab-PTX, which is a PTX protein-bound particle, is frequently used in patients with metastatic PDAC.<sup>2</sup> PTX is a microtubule-stabilizing drug that inhibits cell replication but does not inhibit DNA synthesis in host cells.<sup>36</sup> Microtubule networks are important for adenovirus entry, nuclear tracking, and the development of replication.<sup>37</sup> PTX is also known to affect the instability of microtubules by acetylation and

detyrosination, which is essential for viral internalization and trafficking to the nucleus.<sup>38</sup> Recent papers reported the efficacy of the combination of OAd with PTX.<sup>38,39</sup> Our in vitro virus replication analysis revealed that the only PTX group showed significantly higher VP number than those without chemo. Also, the GEM+PTX group showed significantly higher virus copy number compared to the GEM only group. Furthermore, GEM+nab-PTX+radiation did not hamper virus replication in a hamster syngeneic subcutaneous tumor model. These results indicate that PTX may be suitable for combined use with OAd. To the best of our knowledge, this is the first report evaluating how GEM+nab-PTX+Radiation affects OAd replication in a replication permissive immunocompetent model.

In the colony formation assay, the CI analysis showed that IFN-OAd with GEM+PTX+radiation was synergistic ( $CI<1$ ). As we previously reported, IFN-OAd potentiated the cytotoxicity/antitumor effect of radiation in vitro and in vivo.<sup>18</sup> Type I IFN is known to sensitize many cancers to a variety of chemotherapy and radiation regimens through direct antitumor effects (apoptosis and upregulation of cancer antigens) and indirect antitumor effects (modulation of the immune system, anti-angiogenesis, and alteration in the expression

TABLE 1 Combination index (CI) of the colony formation assay.

	Dose chemo (nM)	Dose radiation (Gy)	Dose virus (VP/cell)	Effect	CI
C+R	2.5	0.625	-	0.754	12.79
	2.5	1.25	-	0.599	0.9563
	2.5	2.50	-	0.422	0.5115
R+V	-	0.625	0.0625	0.562	0.4464
	-	0.625	0.300	0.170	0.3971
	-	0.625	0.625	0.150	0.7211
C+V	2.5	-	0.0625	0.631	1.102
	2.5	-	0.300	0.219	0.8981
	2.5	-	0.625	0.139	1.006
C+R+V	2.5	0.625	0.0625	0.506	0.8775
	2.5	0.625	0.300	0.121	0.6047
	2.5	0.625	0.625	0.063	0.5917

Note: Calculation of the combination index (CI) to determine synergism (CI < 1), antagonism (CI > 1), or additive effect (CI = 1) between virus, chemotherapy, and radiation was performed using Compusyn software.

Abbreviations: C+R+V, chemotherapy+radiation+IFN-OAd; C+R, chemotherapy+radiation; C+V, chemotherapy+IFN-OAd; R+V, radiation+IFN-OAd.

of various oncogenes).<sup>4-7</sup> Furthermore, adenoviral E4 proteins are known to inhibit cellular DNA repair pathways.<sup>40</sup> These factors might contribute to the potentiation of the effect of chemotherapy and radiation therapy, suggesting the possibility of chemotherapy dose reduction in patients with PDAC.

Based on the strong synergy, we decided to use the CRV combination for in vivo experiments. To prove clinical translatability, combination therapy with IFN-OAd must be analyzed in clinically relevant models. While a human cancer xenograft model in immunodeficient mice has been frequently used to evaluate the effect of OAd, it has two problems. One is that murine cells do not permit the replication of human adenovirus,<sup>41</sup> which makes it difficult to assess the replication-induced toxicity. The second issue is that it is impossible to evaluate the immunomodulatory effects of IFN. Therefore, in this study, we aimed to overcome these issues by using the immunocompetent Syrian hamster model,<sup>17</sup> which is capable of supporting the replication of human adenovirus.<sup>42</sup> "CRV" combination significantly suppressed tumor growth compared to CR with no serious side effect, such as weight loss or altered serum biochemistries representing the general condition, liver, and renal function (total protein, albumin, total bilirubin, AST, ALT, BUN, and creatinine). Even though the dose of GEM and nab-PTX was relatively low, CRV showed strong tumor growth suppression. These results suggested that a combination with IFN-OAd may broaden the application of existing chemotherapies to patients who can not tolerate the side effects of chemotherapy by dose reduction.

Analysis of tumor immunity by flow cytometry is a common approach to immune cell profiling and has many benefits, including the characterization of immune cell subsets, quantitative data acquisition, and the ability to examine small subpopulations of interest.<sup>43</sup> However, antibodies that can be used for hamster cells are not well

established to characterize the immune cell subsets. Furthermore, due to the fundamental nature of flow cytometry requiring cell dissociation, histological information (e.g., the distribution and organization of the immune infiltrates or their relationship with other microenvironmental structures) cannot be assessed. To avoid these problems, we asked the pathologist to assess the TIL in both the intratumoral and the marginal areas on HE sections based on the International Immuno-Oncology Biomarker Working Group guidelines for TIL assessment in invasive breast carcinoma.<sup>28,29</sup> According to the guidelines, the marginal area is the 1-mm-wide zone centered on the border of the malignant cells with the host tissue, and the intratumoral area is the central tumor tissue surrounded by this zone.<sup>28,29</sup> In our study, CRV significantly increased the score of TIL in both intratumoral and marginal areas compared to CR. In general, most chemotherapy decreases immune cells,<sup>44</sup> and a higher TIL score is associated with a better prognosis for patients who undergo chemotherapy.<sup>45,46</sup> Furthermore, because the outcome of immune checkpoint inhibitor therapy in patients with cancer has been linked to TIL,<sup>47</sup> IFN-OAd with immunotherapy may show a good combination effect. Publications have reported how OAd activates an antitumor immune response.<sup>48,49</sup> Lytic cell death of cancer cells provides a pro-inflammatory environment and induces an antitumor response. Additionally, IFN can activate the antigen-presenting cells, natural killer (NK) cells, and helper T cells.<sup>7,50</sup> Aoki and colleagues reported that the IFN-expressing replication-deficient adenovirus reduced not only the size of injected tumors but also caused the NK-mediated antitumor efficacy in contralateral non-injected tumors.<sup>51</sup> We tried to assess the CD8+ T cells by using several antibodies that are supposed to be usable for hamster cells. However, they did not work well in our experiments (data not shown). Even though the antibodies specific to hamster cells for immunological analysis are

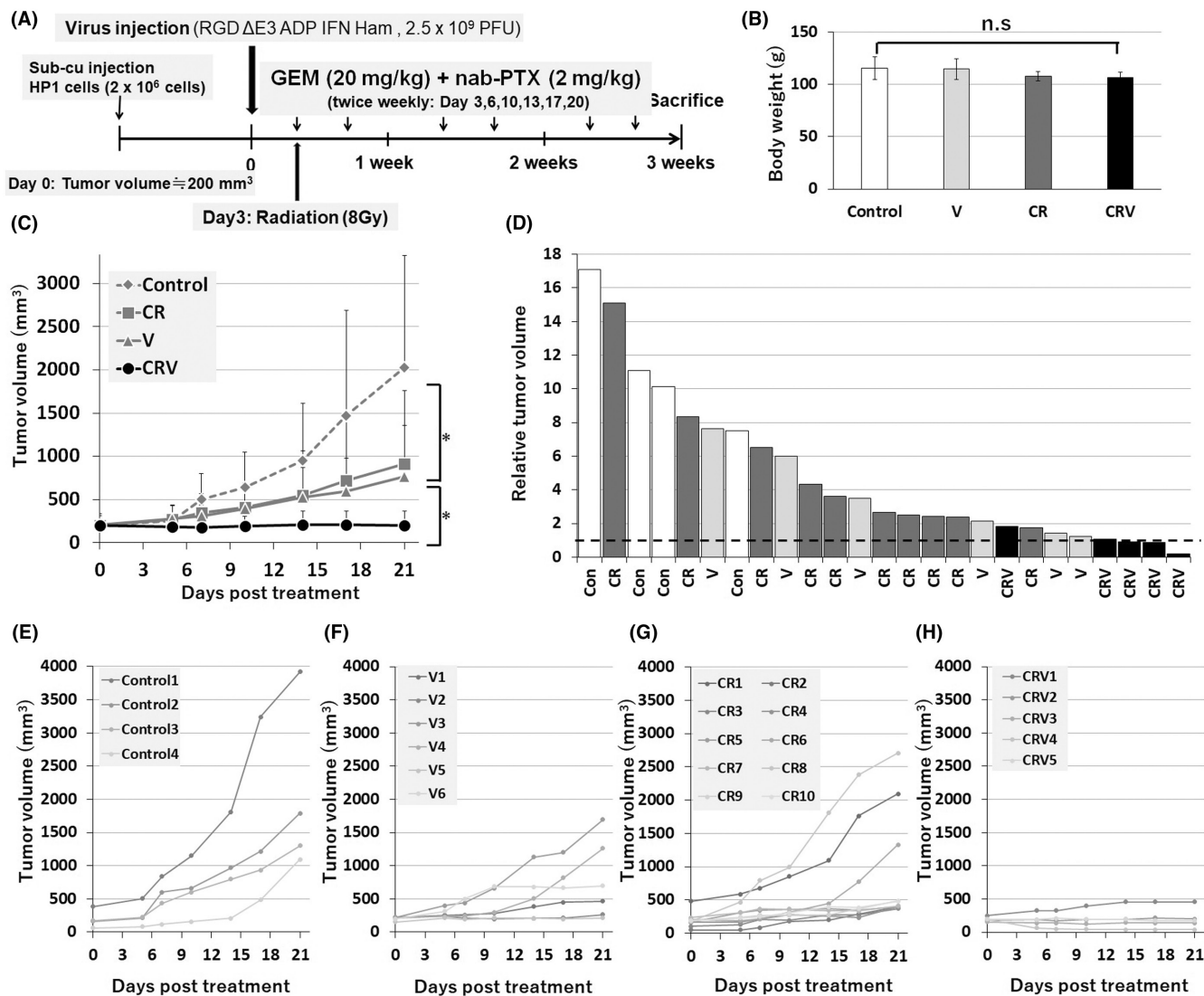


**FIGURE 3** Antitumor effect of interferon (IFN)-expressing oncolytic adenovirus (IFN-OAd) combination therapy in hamster syngeneic subcutaneous tumor model. (A) Treatment schedule for hamsters. HP-1 cells were subcutaneously inoculated. Once the average tumor volume reached  $200\text{ mm}^3$ , the hamsters were divided into four groups: Control ( $n=4$ ), chemotherapy (gemcitabine [GEM] + nab-paclitaxel [nab-PTX]) + radiation (CR) ( $n=10$ ), IFN-OAd (V) ( $n=6$ ), and CRV ( $n=5$ ) groups. A single dose of virus or vehicle alone (PBS) was injected into the tumors on Day 0. Radiation was performed on Day 3. Intraperitoneal injection of  $20\text{ mg/kg}$  GEM +  $2\text{ mg/kg}$  nab-PTX was given twice weekly. (B) The average body weight (g) of each group on Day 21. Data are presented as mean  $\pm$  standard deviation. (C) Average tumor volume of CRV. The average tumor volumes on Day 21 of the control, CR, V, and CRV were  $2027 \pm 1296$ ,  $908 \pm 849$ ,  $767 \pm 593$ , and  $202 \pm 161\text{ mm}^3$ , respectively. (D) Individual relative tumor volume from baseline (Day 0). The dashed line represents the baseline (=1). (E–H) Individual tumor volume of control, CR, V, and CRV. (n.s., not significant; \* $p < 0.05$ ).

**TABLE 2** Serum biochemistries from hamsters on Day 21.

	(Normal ranges)	V	CR	CRV
Total protein (g/dL)	(4.7–7.5)	$6.08 \pm 0.33$	$5.93 \pm 0.36$	$6.08 \pm 0.50$
Albumin (g/dL)	(2.3–4.3)	$3.5 \pm 0.18$	$3.4 \pm 0.34$	$3.5 \pm 0.24$
Total bilirubin (mg/dL)	(0.2–0.8)	$0.18 \pm 0.05$	$0.18 \pm 0.05$	$0.23 \pm 0.05$
AST (U/L)	(28–140)	$68.75 \pm 20.17$	$75.75 \pm 53.66$	$78.00 \pm 20.66$
ALT (U/L)	(27–70)	$40.3 \pm 15.31$	$47.5 \pm 26.34$	$46.0 \pm 43.50$
BUN (mg/dL)	(12–25)	$15.5 \pm 1.73$	$15.5 \pm 1.29$	$17.3 \pm 2.22$
Creatinine (mg/dL)	(0.3–1)	$0.18 \pm 0.10$	$0.10 \pm 0.00$	$0.13 \pm 0.05$

Note: Data are presented as mean  $\pm$  standard deviation ( $n=3$ ).

Abbreviations: V, IFN-OAd; C + R, chemotherapy + radiation; C + R + V, chemotherapy + radiation + IFN-OAd; AST, aspartate aminotransferase; ALT, alanine transaminase; BUN, blood urea nitrogen.



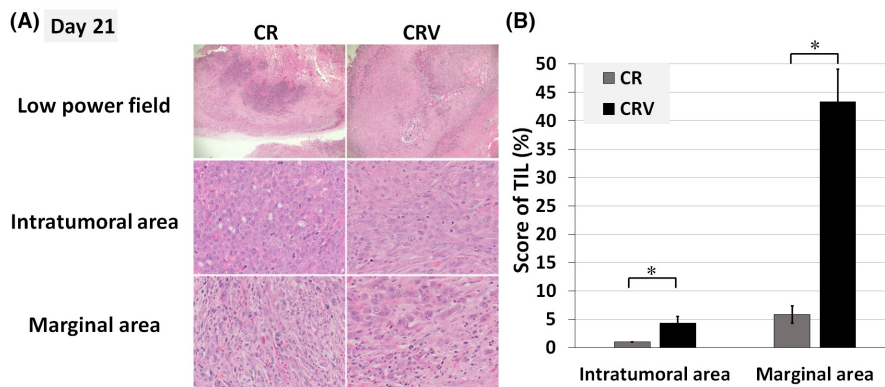


**FIGURE 4** Chemotherapy + radiation + IFN-OAd-induced tumor-infiltrating lymphocytes. (A) Hamster subcutaneous tumors (HP-1 cells) were excised and processed on Day 21 to assess the tumor-infiltrating lymphocyte (TIL). Pathologist assessed the TIL in both the intratumoral and the marginal area on hematoxylin and eosin stain sections based on the International Immuno-Oncology Biomarker Working Group guidelines for TIL assessment in invasive breast carcinoma. (B) After choosing three random areas from both the intratumoral and marginal areas, we scored the average TIL. Necrotic areas were excluded. Data are presented as mean  $\pm$  standard deviation ( $n=3$ ,  $*p<0.05$ , low power field:  $\times 20$  magnifications, intratumoral and marginal area:  $\times 200$  magnifications). CR, chemotherapy (gemcitabine + nab-paclitaxel) + radiation; CRV, CR + IFN-OAd; IFN-OAd, interferon-expressing oncolytic adenovirus.

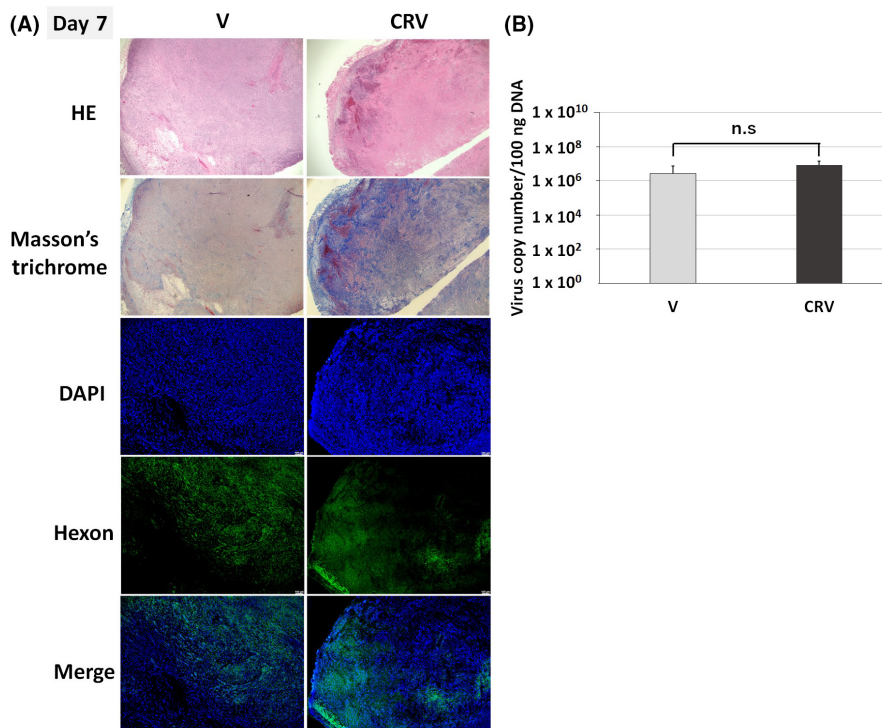


**FIGURE 5** Chemotherapy + radiation did not hamper virus replication in the tumor. (A) Immunological staining of hamster tumors. Under the same therapies (Figure 3A), the hamsters were killed on Day 7. The expression of adenovirus late gene product (hexon) was assessed by immunostaining with the anti-hexon polyclonal antibody (counterstained with DAPI). Green: adenovirus hexon protein; blue: nucleus. HE and Masson's trichrome staining showing the similar region of interest (original magnification:  $\times 20$ ) (B) DNA was purified from whole tumors, and the adenoviral DNA copy number of the E4 region was quantified by quantitative PCR (qPCR). The results are shown as E4 copy number per 100 ng DNA. Data are presented as mean  $\pm$  standard deviation ( $n=3$ ; n.s., not significant). DAPI, 4',6'-diamidino-2-phenylindole; HE, hematoxylin and eosin stain; V, IFN-OAd; CRV, chemotherapy (gemcitabine + nab-paclitaxel) + V.

limited, further research, including the characterization of immune cell subsets and quantitative data acquisition, may help to clarify the immunological modulation of CRV.

In summary, IFN-OAd potentiated the inhibition of radiation and chemotherapy (GEM + PTX) *in vitro* and *in vivo*. In particular, GEM + nab-PTX + radiation + IFN-OAd showed remarkable tumor

inhibition in the hamster syngeneic subcutaneous tumor model without serious side effects. IFN-OAd increased the TIL, and chemoradiation therapy with GEM+nab-PTX+radiation did not hamper IFN-OAd replication in a hamster syngeneic PDAC model that permits human Ad replication. IFN-OAd might overcome the traditional barriers to IFN-based therapy through its tumor-specific expression of IFN, induction of antitumor immunity, and sensitization with chemoradiation. We believe that combining IFN-OAd with GEM+nab-PTX+radiation will be an effective and clinically beneficial treatment for LAPC and BRPC patients.

#### AUTHOR CONTRIBUTIONS

Shuhei Shinoda, Nikita S. Sharma, Naohiko Nakamura, Kazuho Inoko, and Mizuho Sato-Dahlman conducted the experiments. Paari Murugan assessed the TIL on HE sections. Shuhei Shinoda, Julia Davydova, and Masato Yamamoto designed the experiment. Shuhei Shinoda and Masato Yamamoto wrote the paper.

#### ACKNOWLEDGMENTS

We are grateful to Dr. Aoki (National Cancer Research Institute, Tokyo, Japan) for allowing us to use the hamster IFN alpha coding plasmids.

#### FUNDING INFORMATION

This project was partly funded by National Cancer Institute (R01CA228760, R01CA196215, R01CA276480, and P30CA077598-22S3).

#### CONFLICT OF INTEREST STATEMENT

The authors have no commercial associations that might be a conflict of interest in relation to this article.

#### DATA AVAILABILITY STATEMENT

The datasets generated and/or analyzed during the current study are available from the corresponding author upon reasonable request.

#### ETHICS STATEMENT

Approval of the research protocol by an Institutional Reviewer Board: N/A.

Informed consent: N/A.

Registry and the Registration No. of the study/trial: N/A.

Animal studies: All animal study were carried out according to protocols approved by the IACUC of the University of Minnesota.

#### ORCID

Shuhei Shinoda  <https://orcid.org/0000-0002-4128-2177>

#### REFERENCES

- Khalaf N, El-Serag HB, Abrams HR, Thrift AP. Burden of pancreatic cancer: from epidemiology to practice. *Clin Gastroenterol Hepatol*. 2021;19:876-884.
- Park W, Chawla A, O'Reilly EM. Pancreatic cancer: a review. *JAMA*. 2021;326:851-862.
- Siegel RL, Miller KD, Jemal A. Cancer statistics, 2019. *CA Cancer J Clin*. 2019;69:7-34.
- Holsti LR, Mattson K, Niiranen A, et al. Enhancement of radiation effects by alpha interferon in the treatment of small cell carcinoma of the lung. *Int J Radiat Oncol Biol Phys*. 1987;13:1161-1166.
- Ismail A, Van Groeningen CJ, Hardcastle A, et al. Modulation of fluorouracil cytotoxicity by interferon-alpha and -gamma. *Mol Pharmacol*. 1998;53:252-261.
- Morak MJ, van Koetsveld PM, Kanaar R, Hofland LJ, van Eijck CH. Type I interferons as radiosensitisers for pancreatic cancer. *Eur J Cancer*. 2011;47:1938-1945.
- Ma JH, Patrut E, Schmidt J, Knaebel HP, Buchler MW, Marten A. Synergistic effects of interferon-alpha in combination with chemoradiation on human pancreatic adenocarcinoma. *World J Gastroenterol*. 2005;11:1521-1528.
- Picozzi VJ, Kozarek RA, Traverso LW. Interferon-based adjuvant chemoradiation therapy after pancreaticoduodenectomy for pancreatic adenocarcinoma. *Am J Surg*. 2003;185:476-480.
- Nukui Y, Picozzi VJ, Traverso LW. Interferon-based adjuvant chemoradiation therapy improves survival after pancreaticoduodenectomy for pancreatic adenocarcinoma. *Am J Surg*. 2000;179:367-371.
- Schmidt J, Abel U, Debus J, et al. Open-label, multicenter, randomized phase III trial of adjuvant chemoradiation plus interferon Alfa-2b versus fluorouracil and folinic acid for patients with resected pancreatic adenocarcinoma. *J Clin Oncol*. 2012;30:4077-4083.
- Rocha FG, Hashimoto Y, Traverso LW, et al. Interferon-based adjuvant chemoradiation for resected pancreatic head cancer: long-term follow-up of the Virginia Mason protocol. *Ann Surg*. 2016;263:376-384.
- Goradel NH, Mohajel N, Malekshahi ZV, et al. Oncolytic adenovirus: a tool for cancer therapy in combination with other therapeutic approaches. *J Cell Physiol*. 2019;234:8636-8646.
- Sato-Dahlman M, Yamamoto M. The development of oncolytic adenovirus therapy in the past and future - for the case of pancreatic cancer. *Curr Cancer Drug Targets*. 2018;18:153-161.
- Ackrill AM, Foster GR, Laxton CD, Flavell DM, Stark GR, Kerr IM. Inhibition of the cellular response to interferons by products of the adenovirus type 5 E1A oncogene. *Nucleic Acids Res*. 1991;19:4387-4393.
- Sohn SY, Hearing P. Adenoviral strategies to overcome innate cellular responses to infection. *FEBS Lett*. 2019;593:3484-3495.
- Armstrong L, Davydova J, Brown E, Han J, Yamamoto M, Vickers SM. Delivery of interferon alpha using a novel Cox2-controlled adenovirus for pancreatic cancer therapy. *Surgery*. 2012;152:114-122.
- LaRocca CJ, Han J, Gavrikova T, et al. Oncolytic adenovirus expressing interferon alpha in a syngeneic Syrian hamster model for the treatment of pancreatic cancer. *Surgery*. 2015;157:888-898.
- Salzwedel AO, Han J, LaRocca CJ, Shanley R, Yamamoto M, Davydova J. Combination of interferon-expressing oncolytic adenovirus with chemotherapy and radiation is highly synergistic in hamster model of pancreatic cancer. *Oncotarget*. 2018;9:18041-18052.
- Chopra A, Hodges JC, Olson A, et al. Outcomes of neoadjuvant chemotherapy versus chemoradiation in localized pancreatic cancer: a case-control matched analysis. *Ann Surg Oncol*. 2021;28:3779-3788.
- Von Hoff DD, Ervin T, Arena FP, et al. Increased survival in pancreatic cancer with nab-paclitaxel plus gemcitabine. *N Engl J Med*. 2013;369:1691-1703.
- Hara H, Kobayashi A, Yoshida K, et al. Local interferon-alpha gene therapy elicits systemic immunity in a syngeneic pancreatic cancer model in hamster. *Cancer Sci*. 2007;98:455-463.
- Doronin K, Toth K, Kuppuswamy M, Krajcsi P, Tollefson AE, Wold WS. Overexpression of the ADP (E3-11.6K) protein increases cell lysis and spread of adenovirus. *Virology*. 2003;305:378-387.

23. Dmitriev I, Krasnykh V, Miller CR, et al. An adenovirus vector with genetically modified fibers demonstrates expanded tropism via utilization of a coxsackievirus and adenovirus receptor-independent cell entry mechanism. *J Virol*. 1998;72:9706-9713.
24. Davydova J, Le LP, Gavrikova T, Wang M, Krasnykh V, Yamamoto M. Infectivity-enhanced cyclooxygenase-2-based conditionally replicative adenoviruses for esophageal adenocarcinoma treatment. *Cancer Res*. 2004;64:4319-4327.
25. Miura Y, Yamasaki S, Davydova J, et al. Infectivity-selective oncolytic adenovirus developed by high-throughput screening of adenovirus-formatted library. *Mol Ther*. 2013;21:139-148.
26. Hall EJ, Giaccia AJ. *Radiobiology for the Radiologist*. 8th ed. Wolters Kluwer; 2019:597.
27. Chou TC. Theoretical basis, experimental design, and computerized simulation of synergism and antagonism in drug combination studies. *Pharmacol Rev*. 2006;58:621-681.
28. Salgado R, Denkert C, Demaria S, et al. The evaluation of tumor-infiltrating lymphocytes (TILs) in breast cancer: recommendations by an international TILs Working group 2014. *Ann Oncol*. 2015;26:259-271.
29. Hendry S, Salgado R, Gevaert T, et al. Assessing tumor-infiltrating lymphocytes in solid tumors: a practical review for pathologists and proposal for a standardized method from the international Immunooncology biomarkers Working group: part 1: assessing the host immune response, TILs in invasive breast carcinoma and ductal carcinoma in situ, metastatic tumor deposits and areas for further research. *Adv Anat Pathol*. 2017;24:235-251.
30. Yamamoto M, Davydova J, Wang M, et al. Infectivity enhanced, cyclooxygenase-2 promoter-based conditionally replicative adenovirus for pancreatic cancer. *Gastroenterology*. 2003;125:1203-1218.
31. Dilley J, Reddy S, Ko D, et al. Oncolytic adenovirus CG7870 in combination with radiation demonstrates synergistic enhancements of antitumor efficacy without loss of specificity. *Cancer Gene Ther*. 2005;12:715-722.
32. Omori T, Tazawa H, Yamakawa Y, et al. Oncolytic virotherapy promotes radiosensitivity in soft tissue sarcoma by suppressing anti-apoptotic MCL1 expression. *PLoS One*. 2021;16:e0250643.
33. Saha B, Parks RJ. Identification of human adenovirus replication inhibitors from a library of small molecules targeting cellular epigenetic regulators. *Virology*. 2021;555:102-110.
34. Onimaru M, Ohuchida K, Egami T, et al. Gemcitabine synergistically enhances the effect of adenovirus gene therapy through activation of the CMV promoter in pancreatic cancer cells. *Cancer Gene Ther*. 2010;17:541-549.
35. Weber HL, Gidekel M, Werbach S, et al. A novel CDC25B promoter-based oncolytic adenovirus inhibited growth of Orthotopic human pancreatic tumors in different preclinical models. *Clin Cancer Res*. 2015;21:1665-1674.
36. Nawara HM, Afify SM, Hassan G, Zahra MH, Seno A, Seno M. Paclitaxel-based chemotherapy targeting cancer stem cells from mono- to combination therapy. *Biomedicine*. 2021;9:9.
37. Flatt JW, Butcher SJ. Adenovirus flow in host cell networks. *Open Biol*. 2019;9:190012.
38. Hossain E, Habiba U, Yanagawa-Matsuda A, et al. Advantages of using paclitaxel in combination with oncolytic adenovirus utilizing RNA destabilization mechanism. *Cancers (Basel)*. 2020;12:12.
39. Ishikawa W, Kikuchi S, Ogawa T, et al. Boosting replication and penetration of oncolytic adenovirus by paclitaxel eradicate peritoneal metastasis of gastric cancer. *Mol Ther Oncolytics*. 2020;18:262-271.
40. Boyer J, Rohleder K, Ketner G. Adenovirus E4 34k and E4 11k inhibit double strand break repair and are physically associated with the cellular DNA-dependent protein kinase. *Virology*. 1999;263:307-312.
41. Duncan SJ, Gordon FC, Gregory DW, et al. Infection of mouse liver by human adenovirus type 5. *J Gen Virol*. 1978;40:45-61.
42. Thomas MA, Spencer JF, La Regina MC, et al. Syrian hamster as a permissive immunocompetent animal model for the study of oncolytic adenovirus vectors. *Cancer Res*. 2006;66:1270-1276.
43. Young YK, Bolt AM, Ahn R, Mann KK. Analyzing the tumor microenvironment by flow cytometry. *Methods Mol Biol*. 2016;1458:95-110.
44. Schmidt T, Jonat W, Wesch D, et al. Influence of physical activity on the immune system in breast cancer patients during chemotherapy. *J Cancer Res Clin Oncol*. 2018;144:579-586.
45. Adams S, Gray RJ, Demaria S, et al. Prognostic value of tumor-infiltrating lymphocytes in triple-negative breast cancers from two phase III randomized adjuvant breast cancer trials: ECOG 2197 and ECOG 1199. *J Clin Oncol*. 2014;32:2959-2966.
46. Kiryu S, Ito Z, Suka M, et al. Prognostic value of immune factors in the tumor microenvironment of patients with pancreatic ductal adenocarcinoma. *BMC Cancer*. 2021;21:1197.
47. Paijens ST, Vledder A, de Bruyn M, Nijman HW. Tumor-infiltrating lymphocytes in the immunotherapy era. *Cell Mol Immunol*. 2021;18:842-859.
48. Li X, Wang P, Li H, et al. The efficacy of oncolytic adenovirus is mediated by T-cell responses against virus and tumor in Syrian hamster model. *Clin Cancer Res*. 2017;23:239-249.
49. Liikanen I, Ahtiainen L, Hirvonen ML, et al. Oncolytic adenovirus with temozolomide induces autophagy and antitumor immune responses in cancer patients. *Mol Ther*. 2013;21:1212-1223.
50. Marrack P, Kappler J, Mitchell T. Type I interferons keep activated T cells alive. *J Exp Med*. 1999;189:521-530.
51. Ohashi M, Yoshida K, Kushida M, et al. Adenovirus-mediated interferon alpha gene transfer induces regional direct cytotoxicity and possible systemic immunity against pancreatic cancer. *Br J Cancer*. 2005;93:441-449.

**How to cite this article:** Shinoda S, Sharma NS, Nakamura N, et al. Interferon-expressing oncolytic adenovirus + chemoradiation inhibited pancreatic cancer growth in a hamster model. *Cancer Sci*. 2023;114:3759-3769. doi:[10.1111/cas.15903](https://doi.org/10.1111/cas.15903)